Int. J. Nano Dimens., 12 (1): 67-75, Winter 2021

ORIGINAL ARTICLE

Synthesis and characterization of $Mg1_{-x}Ni_xAl_2O_4$ and their photocatalytic behaviors towards Congo red under UV light irradiation

Reza Hajavazzade [1], Maryam Kargar Razi [1,*], Ali Reza Mahjoub [2]

[1]Department of chemistry, Tehran North Branch, Islamic Azad University, Tehran, Iran
[2] Department of Chemistry, Faculty of Science, Tarbiat Modares University Tehran, Iran

Received 10 June 2020; revised 06 September 2020; accepted 07 September 2020; available online 20 September 2020

Abstract

In this paper, $MgAl_2O_4$ nanoparticles were synthesized by the Sol-gel auto combustion method and were doped with different concentrations of Ni^{2+} (x= 0, 0.1, 0.05, and 0.03). By this method, a novel photocatalyst which had better decolorization percentages of Congo red $_{compared}$ to $MgAl_2O_4$ was produced. The $MgAl_2O_4$ samples were calcinated at 1000 ^{0}C. The samples obtained were characterized by X-ray diffraction (XRD), SEM, FT-IR, EDX, and ICP-AES. The photocatalytic activity of $MgAl_2O_4$ samples were evaluated by UV-Vis spectroscopy and diffuse reflectance spectra (DRS) to confirm the performance rate of the photocatalyst. Also, the photocatalytic properties were investigated in the presence of UV light, certain amounts of photocatalysts, and Congo red dye. The best- obtained results of the photocatalytic activity among the prepared samples were $Mg_{0.9}Ni_{0.1}Al_2O_4$ because this photocatalyst had a removal conversion of 99.3 % of the dye after 90 min, which was better than other photocatalysts in similar conditions. $Mg_{0.9}Ni_{0.1}Al_2O_4$ was used as a photocatalyst five successfully times without any changes or loss of its high photocatalytic activity for this process. In this project, we used Ni^{2+} to dope $MgAl_2O_4$ nanoparticles. The results decolorization percentages of Congo red showed that $Mg_{0.9}Ni_{0.1}Al_2O_4$ had better efficiency compared to $MgAl_2O_{4,\ and\ other}$ photocatalysts.

Keywords: *Congo Red; $MgAl_2O_4$; Nanoparticles; Photocatalyst; Sol-gel Auto Combustion Method.*

How to cite this article

Hajavazzade R., Kargar Razi M. Mahjoub A.R. Synthesis and characterization of Mg1-x$Ni_xAl_2O_4$ and their photocatalytic behaviors towards Congo red under UV light irradiation. Int. J. Nano Dimens., 2020; 12(1): 67-75.

INTRODUCTION

In recent years, extensive attention has been paid to environmental problems. Photocatalysis technology is a useful strategy for solving the energy and environment issues due to the generation of photo-induced electrons and holes through light irradiating on the photocatalysts that would simplify the removal of pollutants in water, air, and organic synthesis [1-2]. Some of the dyes such as azo dyes are used for their high performance in metallurgy, carpet, paper, textile, and leather industries. Azo dyes are toxic, stable in nature; they have high thermal stability, carcinogenicity, and many detrimental effects on human health, aquatic systems, and animals [3]. Congo red is some type of the anionic synthetic dyes which has two azo (–N=N–) chromophores. This compound is more stable than other azo dyes, because of its complex aromatic structure [4]. Recently, many scientists have been attempting to eliminate these pollutants. Available methods for removal of azo dyes include chemical oxidation, coagulation [5], adsorption, and electrochemical processes [6]. These methods are not effective for removal of the mentioned organic materials from industrial wastes [7] since in these methods; photocatalytic processes are very slow at high concentrations or rather ineffective at very low amounts of contaminants. Also, the contaminant changes from one phase to another phase. Among

* Corresponding Author Email:
m_kargarrazi@iau-tnb.ac.ir

Table 1. Different amounts of reagents in synthesis $Mg_{1-x}Ni_xAl_2O_4$ of by sol-gel auto combustion method.

x valve	$Mg(NO_3)_2.6H_2O$ (mmol)	$Ni(NO_3)_2.6H_2O$ (mmol)	$Al(NO_3)_2.9H_2O$ (mmol)
x= 0	7.8	0	15.6
x= 0.1	7.02	0.78	15.6
x= 0.05	7.41	0.39	15.6
x= 0.03	7.566	0.234	15.6

all these methods, photocatalytic technology has attracted much attention through employing the semiconductors for the water treatment because of their functions in green chemistry, their nontoxicity, their energy-conserving applications, and low-cost functionality, as it employs only UV and Visible light to decompose pollutants [8-17]. Spinel oxides with the general chemical formula of AB_2O_4, A, and B are two different cations with different oxidation numbers. A is a divalent ion and B is a trivalent ion. They have been used as ceramics, optical materials, catalysts, and photocatalysts because of their unique properties [18, 19]. Several spinels are semiconductor materials that have been used in photocatalytic removal of pollutants or photocatalytic composition in water. The great benefit of this material is that their band gaps and other properties can be handled easily.

Magnesium aluminate spinel ($MgAl_2O_4$) is one of the most important oxidizing spinels and ceramic materials that has good mechanical properties and encompasses a wide range of applications that can tolerate very high temperatures [20-21]. Since it has a very high melting temperature (2135 ^{0}C), it is resistant to mechanical stress, and thermal shock, at room temperature and higher temperatures. Also, its unique optical properties and low dielectric constant provide special applications for the spinel. Recently, $MgAl_2O_4$ has been received attention as a photocatalyst and many research groups have studied and used it as a photocatalyst on different materials [22, 23]. Magnesium aluminate spinel has a relatively high band gap as a semiconductor. It can be used to reduce the band gap and improve photocatalytic properties by doping these nanoparticles with metals such as Ni^{2+}, Cu^{2+}, and Zn^{2+}.

Different methods such as sol–gel [24, 25], co-precipitation [26], solid state method, have been reported for the synthesis of ($MgAl_2O_4$). Among these methods, sol–gel, and co-precipitation are very common. Due to it can produce smaller nanoparticles and requires a lower synthesis temperature compared to other methods. Using a hybrid sol–gel combustion method at relatively low temperature is a new method to produce magnesium aluminate nanoparticles suitable for different applications, especially the photocatalytic.

In this study, Magnesium aluminate spinel ($MgAl_2O_4$) nanoparticles were synthesized and doped with different mass percentages of Ni^{2+} by using the sol-gel auto combustion method. These nanoparticles were used as a photocatalyst for the removal of Congo red dye. Photocatalytic activity of these materials was studied under UV light radiation for Congo red, with magnesium aluminate spinel doped with different percentages of Ni^{2+} for 90 minutes.

EXPERIMENTAL

Materials and methods

All chemicals were purchased from Merck or Sigma-Aldrich with the analytical grade. Fourier transform infrared (FT-IR) spectra were obtained using the FT BOMEM MB102 IR spectrophotometer. X-ray diffraction (XRD) patterns of the synthesized samples were obtained with a Philips X-ray diffractometer (model PW1730). The SEM and EDX images were obtained by Hitachi Scanning Electron Microscope. The photocatalytic reactions were performed using a photoreactor in which four UV lamps with λ_{max}= 254 nm, manufactured by Holland (UV-C, 6 W, PHILIPS) were operated.

Preparation of nanoparticles

The analytical grades of 6.8 mmol magnesium nitrate $Mg(NO_3)_2.6H_2O$, 6 mmol aluminum nitrate $Al(NO_3)_2.9H_2O$, and different percentages of nickel nitrate $Ni(NO_3)_2$ were dissolved in 5 ml of distilled water and stirred at 60 ^{0}C for 10 minutes. The quantities of nickel nitrate Ni $(NO_3)_2.6H_2O$ are shown in Table 1. After that, 44.25 mmol of urea was dissolved in 25 ml of distilled water and added to this mixture and refluxed at 80 ^{0}C for 1 hour and then refluxed at 120 ^{0}C for 5 hours.

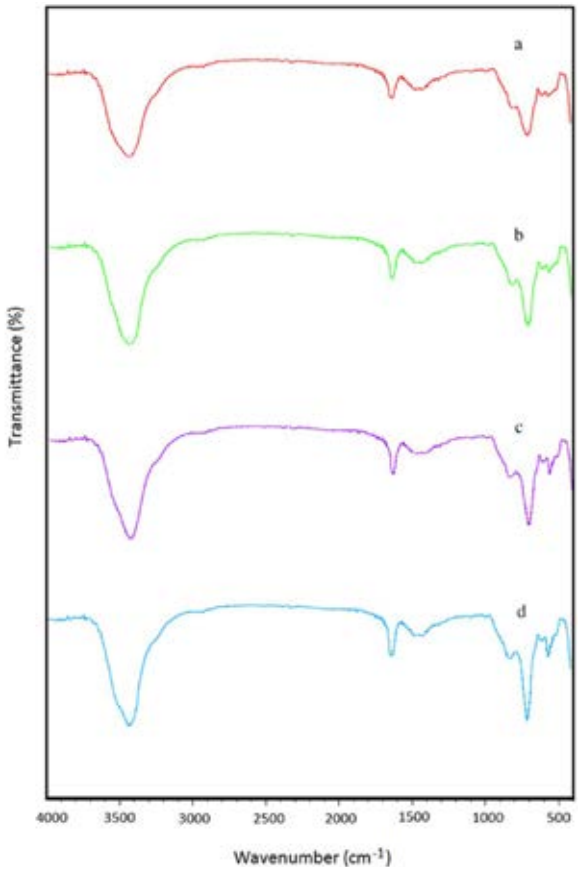

Fig. 1. FT-IR spectra of $MgAl_2O_4$ (a): x=0, (b): x=0.03, (c): x=0.05, (d): x=0.1.

It was then cooled slowly at room temperature and was placed for 2 hours at 200 ^{0}C in an oven and then calcined at 1000 ^{0}C for 4 hours [27]. The photocatalytic activity of the synthesized spinel catalyst was assessed by monitoring the removal of the Congo red solution under the UV light irradiation. A UV lamp was used as the UV light source and was positioned parallel to the quartz tube. In each experiment, 0.1 g of the catalyst was dispersed in 50 mL of Congo red solutions with a concentration of 10 mg/L, at room temperature. To earn the adsorption/desorption equilibrium, the suspensions were stirred in a dark room and ultrasonic bath for 30 min before the irradiation. During the irradiation process, stirring was continued to hold the mixture in the suspension form. At given time intervals, around 2 mL of the suspension was taken every 10 minutes and centrifuged to remove the photocatalyst. After that, the solution was analyzed by UV-Vis spectrophotometry at a wavelength of 505 nm. The decolorization rate D was calculated by equation (1), where C_0 is the absorbance of the first solution, and C is the absorbance of the solution at different times, and different irradiation.

$$D= A_0\text{-}A/A_0 \times 100 \quad (1)$$

RESULTS AND DISCUSSION

FT-IR spectra

$MgAl_2O_4$ was prepared by sol-gel auto combustion method. The FT-IR spectra of $MgAl_2O_4$ and $Mg_{1-X}Ni_XAl_2O_4$ (x= 0.1, 0.05, 0.03) are presented in Fig.1. (see Fig.1 a, b, c, d). In the IR spectra, the $MgAl_2O_4$ samples displayed two stretching bands at 555 cm^{-1} and 700 cm^{-1} consecrated to the [AlO_6] groups, the vibration of Mg–O stretching, and displaying the formation of $MgAl_2O_4$ spinel. Peak intensity increased at 700 cm^{-1} and 555 cm^{-1} [28, 29] with increasing nickel, which indicates that the crystalline properties of the samples increase. The absorption spectra in the region of 1630 cm^{-1} and 3437 cm^{-1} are the bending vibrations associated with water [30].

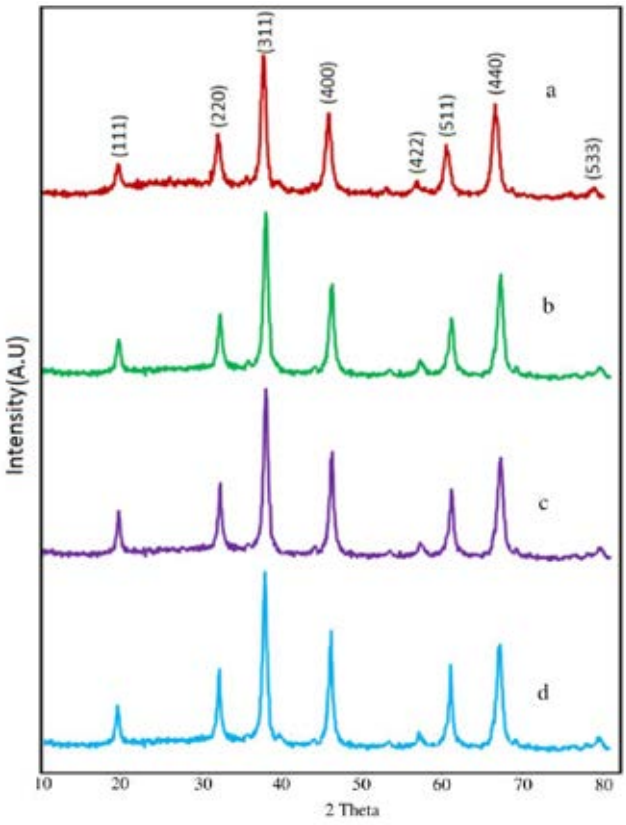

Fig. 2. XRD patterns of $MgAl_2O_4$ (a): x=0, (b): x=0.03, (c): x=0.05, (d): x=0.1.

X-ray diffraction

The XRD patterns of $MgAl_2O_4$ and $Mg_{1-X}Ni_XAl_2O_4$ are shown in Fig.2 a, b, c, d. The pattern of magnesium aluminate spinel with the standard card (JCPDS card no. 01-075-1798), indicates the retention of the spinel structure of $MgAl_2O_4$ during the doping with Ni^{2+}. The diffraction peaks related to Bragg's reflections from (111), (220), (311), (400), (422), (511), (440), and (533) planes correspond to the standard spinel structure of $MgAl_2O_4$. No extra peaks of the phase have been observed, in following the standard X-ray powder diffraction pattern of magnesium aluminate spinel. The crystallite size of $MgAl_2O_4$ nanoparticles was about 40 nm, as determined by using the Debye–Scherrer formula. As indicated in Fig 2. the intensity of peaks related to (220), (311), (400), and (511) planes increases with the increase in the amount of Ni^{2+} substitutions in comparison with the $MgAl_2O_4$ and $Mg_{1-X}Ni_XAl_2O_4$ indicating the formation of the $Mg_{1-X}Ni_XAl_2O_4$ solid solution and the increase in the crystallinity of the samples [31, 32].

Scanning Electron Microscopy (SEM)

SEM images of magnesium aluminate spinel nanoparticles, $Mg_{0.97}Ni_{0.03}Al_2O_4$, $Mg_{0.95}Ni_{0.05}Al_2O_4$, $Mg_{0.9}Ni_{0.1}Al_2O_4$, are shown in Fig. 3 a, b, c, d. According to the SEM images, magnesium aluminate spinel nanoparticles have the spherical morphology and are uniform. SEM images of magnesium aluminate spinel nanoparticles doped with nickel are shown in Fig.3 [33, 34]. Magnesium aluminate spinel nanoparticles retain their spherical morphology and have a good quality despite being doped with Ni^{2+}(Fig. 3 b, c, d). The EDX pattern of magnesium aluminate spinel doped with 4% nickel is shown in Fig.4. As indicated in Fig 4, the atoms of Mg, Al, O, and Ni are shown in various percentages, and the data obtained for nickel match the expected values. The amount of Ni^{2+} in $Mg_{0.97}Ni_{0.03}Al_2O_4$, $Mg_{0.95}Ni_{0.05}Al_2O_4$, $Mg_{0.9}Ni_{0.1}Al_2O_4$ was determined by the ICP-AES analysis to be 2.98, 4.99, 9.98 mol%.

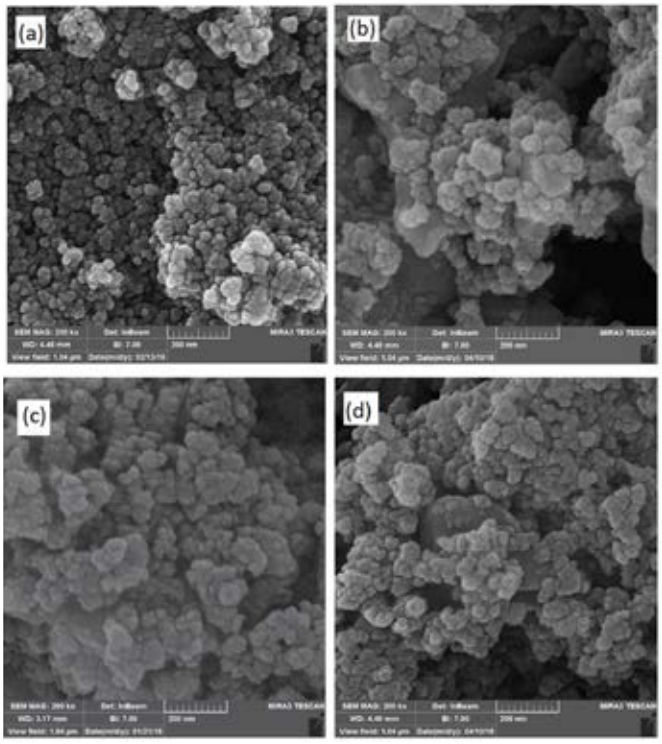

Fig. 3. SEM images of $MgAl_2O_4$ (a): x=0, (b): x=0.03, (c): x=0.05, (d): x=0.1.

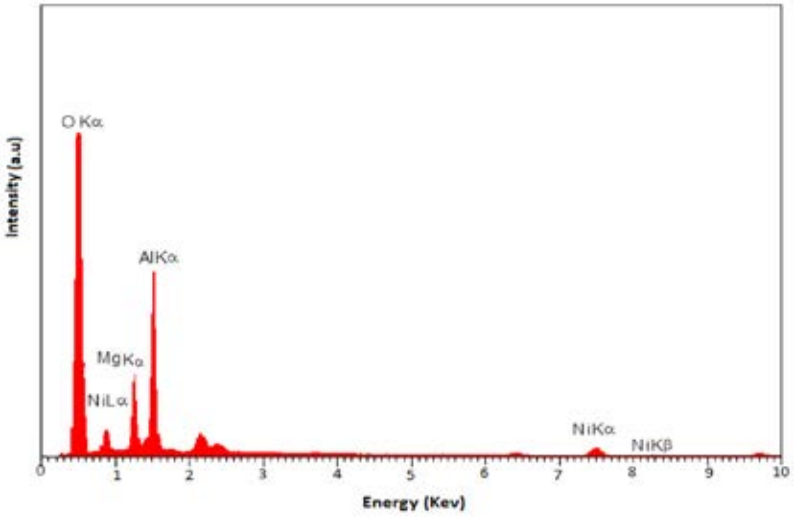

Fig. 4. EDX spectrum of $Mg_{0.9}Ni_{0.1}Al_2O_4$.

Photocatalytic activity of $Mg_{1-x}Ni_xAl_2O_4$ spinel powders

As indicated in Fig. 5 a, b, c, d. Congo red dye cannot be decolorized under visible light irradiation in the absence of photocatalysts. It can be seen that Congo red is very stable and no serious decolorization is observed after the visible light irradiation exposure. The concentration of Congo red dye dramatically decreases with the increasing irradiation time, as soon as the photocatalysts were added. The absorption of the samples shows a decrease in the concentration of Congo red solution in the presence of the catalyst. The best result for decolorization of Congo red was calculated by (1) after 90 min of exposure to the UV light irradiation by using, 50 mL of Congo

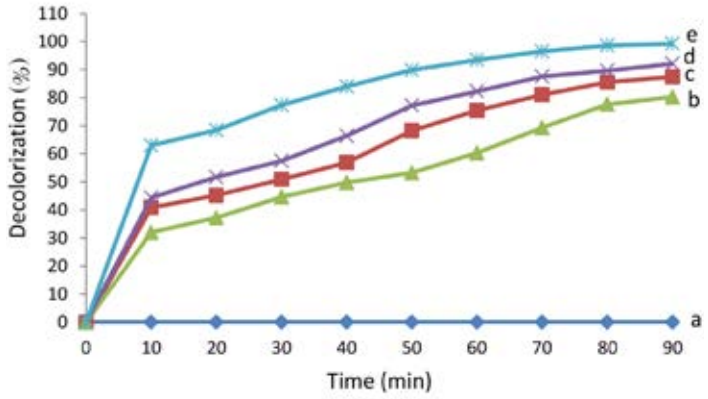

Fig. 5. Decolorization rate of the Congo red dye solution under UV light irradiation using the $Mg_{1-x}Ni_xAl_2O_4$ spinel powders prepared (a): without catalyst, (b): x=0, (c): x=0.03, (d): x=0.05, (e): x=0.1.

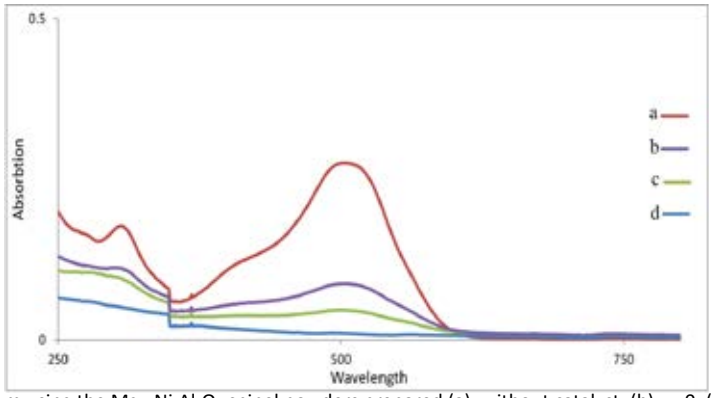

Fig. 6. UV–Vis spectrum using the $Mg_{1-x}Ni_xAl_2O_4$ spinel powders prepared (a): without catalyst, (b): x=0, (c): x=0.05, (d): x=0.1.

red solution 10 mg/L, and $Mg_{0.9}Ni_{0.1}Al_2O_4$ with decolorization of 99.3%. To remove the Congo red, 0.1 g from $Mg_{0.9}Ni_{0.1}Al_2O_4$ was used, which demonstrated a yield of 99.3%, while showed a higher efficiency compared to magnesium aluminate spinel and others with similar conditions (Fig. 6). The Results of this project are compared with similar researches (Table 2).

DRS spectra

The DRS spectra of $MgAl_2O_4$, $Mg_{0.97}Ni_{0.03}Al_2O_4$, $Mg_{0.95}Ni_{0.05}Al_2O_4$, and $Mg_{0.9}Ni_{0.1}Al_2O_4$ are presented in Fig. 7 a, b, c, d. The band that is displayed next to the visible light region for each spectrum perhaps can be attributed to the $O_2 \rightarrow Al^{3+}$ charge transition because of the excitation of electrons from the valence band of O (2p) to the transference band of Al (3d). The band gap energy of the synthesized photocatalysts can be calculated according to the formula Eg=1240/λ . Eg is the band gap energy and λ is the absorption edge. The optical band gap energy values are 4.42, 4.27, 4.13, and 4.07 eV for $MgAl_2O_4$, $Mg_{0.97}Ni_{0.03}Al_2O_4$, $Mg_{0.95}Ni_{0.05}Al_2O_4$, and synthesized $Mg_{0.9}Ni_{0.1}Al_2O$. When Ni^{2+} was added to $MgAl_2O_4$ the orbitals between $Ni3d^8$ and O2p were hybridized, due to the $Ni3d^8$ orbitals were filled with eight electrons. The replacement of Ni^{2+} with Mg^{2+} has improved the photocatalytic activity of magnesium aluminate spinel [39, 40].

Recovering of the catalyst

The $Mg_{0.9}Ni_{0.1}Al_2O$ was isolated from the final product by simple filtration. After that, the catalyst was washed several times with water. It was reused in a new reaction after drying. The recovered catalyst could be reused five times with no changes in the photocatalytic activity. The FT-IR spectrum of the recovered catalyst shows that it has been used for five successive times (Fig. 8). The results are listed in Fig 9.

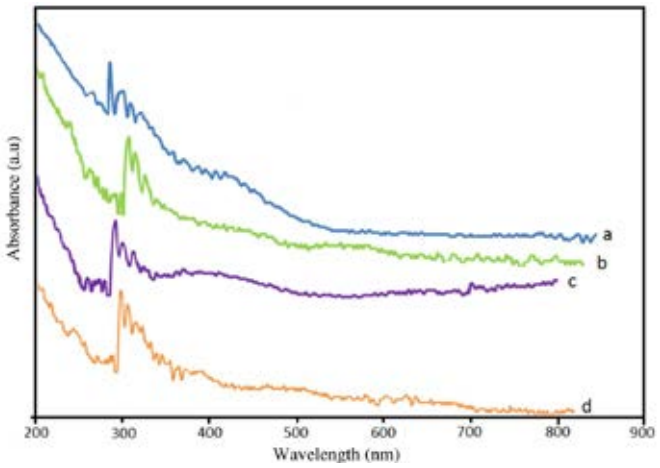

Fig. 7. UV–Vis diffuse reflectance spectra of $Mg_{1-x}Ni_xAl_2O_4$ spinel powders prepared (a): x=0, (b): x=0.1, (c): x=0.03, (d): x=0.05.

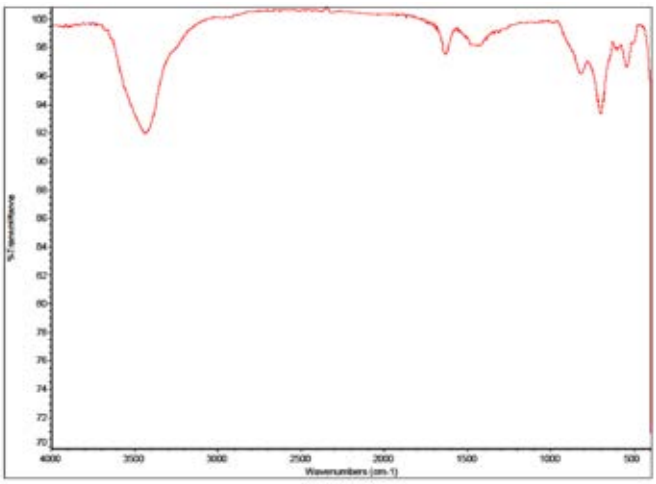

Fig. 8. FT-IR spectra of $Mg_{0.9}Ni_{0.1}Al_2O_4$ recycled after the fifth Run.

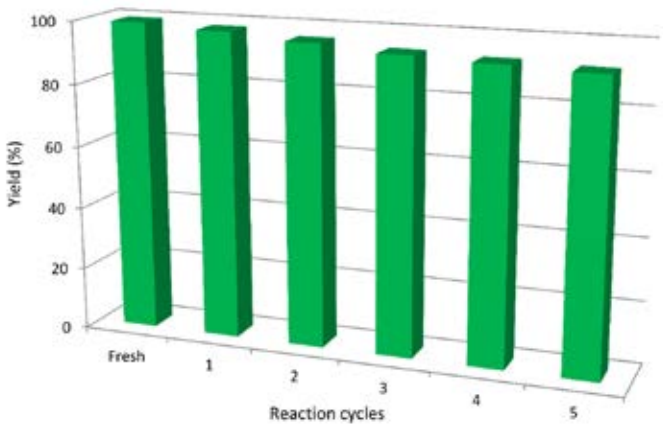

Fig. 9. Reusability of $Mg_{0.9}Ni_{0.1}Al_2O_4$ for decolorization of Congo red.

Table 2. CR removal by different photocatalysts.

Entry	Photocatalyst	Pollutant	Time (min)	Removal (%)	Ref
1	Alginate/ C-Fe_2O_3/CdS	20 mg/L	300	91	[35]
2	$ZnFe_2O_4$/Graphene	15 mg/L	270	88	[36]
3	ZnS-CdS	50 mg/L	60	98	[37]
4	Nb–O–Mo	10 mg/L	240	99	[38]
5	$Mg_{0.9}Ni_{0.1}Al_2O_4$	10 mg/L	90	99/3	This work

CONCLUSION

In this study, $MgAl_2O_4$ nanoparticles were produced by sol-gel auto combustion method and were doped with different mass percentages of Ni^{2+} (x= 0, 0.1, 0.05, and 0.03). The prepared nanoparticles were characterized by X-ray diffraction (XRD), SEM, FT-IR, EDX, and ICP-AES. These nanoparticles were used as a catalyst for decolorization of Congo red 10 mg/L solution in the presence of UV light. The nanoparticles used in this reaction have the potential to be used in the degradation of Congo red. The results showed that $Mg_{0.9}Ni_{0.1}Al_2O_4$ had better decolorization percentages of Congo red compared to $MgAl_2O_4$, $Mg_{0.95}Ni_{0.05}Al_2O_4$, and, $Mg_{0.97}Ni_{0.03}Al_2O_4$ with UV light irradiation using a 0.1g catalyst and, 50 mL of Congo red solution 10 mg/L after 90 min. The efficiency of the photocatalyst ($Mg_{0.9}Ni_{0.1}Al_2O_4$) with similar papers for decolorization of Cong red was compared. The results show the high efficiency of the photocatalyst.

ACKNOWLEDGMENT

Financial support of this paper by Tehran North Branch, Islamic Azad University, and Tarbiat Modares University, is thankfully acknowledged. Reza Hajavazzade Ph.D. student who did all the experience. Maryam Kargar Razi; Supervisor of the project. Alireza Mahjoub; Advisor of the project.

CONFLICT OF INTEREST

The authors declare that there is no conflict of interest.

REFERENCES

1. Selcuk S., Selloni A., (2016), Facet-dependent trapping and dynamics of excess electrons at anatase TiO_2 surfaces and aqueous interfaces. *Nature Mater.* 15: 1107–1112.
2. Xu Y., Huang Y., Zhang B., (2016), Rational design of semiconductor-based photocatalysts for advanced photocatalytic hydrogen production: The case of cadmium chalcogenides. *Inorg. Chem. Fron.* 3: 591–615.
3. Sakkas V. A., Islam M. A., Stalikas C., Albanis T. A., (2010), Photocatalytic degradation using design of experiments: A review and example of the Congo red degradation. *J. Hazard. Mater.* 175: 33–44.
4. Ramakrishnan R., Kalaivani S., Joice J. A. I., Sivakumar T., (2012), Photocatalytic activity of multielement doped TiO_2 in the degradation of congo red. *Appl. Surf. Sci.* 258: 2515-2521.
5. Verma A. K., Dash R. R., Bhunia P., (2012), A review on chemical coagulation/flocculation technologies for removal of colour from textile wastewaters. *J. Envir. Manage.* 93: 154–168.
6. Zhu X. P., Ni J. R., Wei J. J., Xing X., Li H., (2011), Destination of organic pollutants during electrochemical oxidation of biologically-pretreated dye wastewater using boron-doped diamond anode. *J. Hazard. Mater.* 189: 127–133.
7. Hassani A., Alidokht L., Khataee A. R., Karaca S., (2014), Optimization of comparative removal of two structurally different basic dyes using coal as a low-cost and available adsorbent. *J. Taiw. Inst. Chem. Engin.* 45: 1597–1607.
8. Younes S. B., Cherif I., Dhouib A., Sayad S., (2015), Trametes trogii: A biologic powerful tool for dyes decolorization and detoxification. *Catal. Lett.* 146: 204-211.
9. Rasouli N., Salavati H., Movahedi M., Rezaei A., (2017), An Insight on kinetic adsorption of Congo red dye from aqueous solution using magnetic chitosan based composites as Adsorbent. *Chem. Methodol.* 1: 74-86.
10. Salavati H., Teimouri A., Kazemi S., (2017), Synthesis and characterization of novel composite-based phthalocyanine used as efficient photocatalyst for the degradation of methyl orange. *Chem. Methodol.* 1: 12-27.
11. Eldefrawy M., Gomaa E. G. A., Salem S., Abdel Razik F., (2018), Cyclic voltammetric studies of calcium acetate salt with methylene blue (MB) using gold electrode. *Pro. Chem. Biochem. Res.* 1: 11-18.
12. Simsek E. B., Demircivi P., Berek D., Novak I., (2017), Fabrication of carbon fiber supported zirconium titanium nanocomposites for efficient photocatalytic decolorization of Orange II dye under visible light irradiation. *React. Kinet. Mech. Cat.* 124: 89-99.
13. Singh R., Kumar M., Khajuria H., Ladol J., Sheikh H. N., (2018), Hydrothermal synthesis of magnetic Fe_3O_4 Nitrogen doped grapheme hybrid composite and its application as photocatalyst in degradation of methyl orange and methylene blue dyes in presence of copper (II) ions. *Chem.*

Paper. 72: 1181-1192.
14. Zaccaria S., Boff N. A., Bettin F., Pinheiro Dillon A. J., (2019), Use of micro- and ultrafiltration membranes for concentration of laccase-rich enzymatic extract of Pleurotus sajor-caju PS-200 and application in dye decolorization. *Chem. Paper.* 73: 3085-3093.
15. Thomas O. E., Adegoke O. A., Kazeem A. F., Ezeuchenne I. C., (2019), Preferential solvation of mordant black and solochrome dark blue in mixed solvent systems. *Prog. Chem. Biocheml. Rese.* 2: 40-52.
16. Rahimian R., Zarinabadi S., (2020), A review of studies on the removal of methylene blue dye from industrial wastewater using activated carbon adsorbents made from almond bark. *Prog. Chem. Biochem. Res*. 3: 251-268.
17. Rezayati zad Z., Moosavi B., Taheri A., (2020), Synthesis of monodisperse magnetic hydroxyapatite/Fe_3O_4 nanospheres for removal of Brilliant Green (BG) and Coomassie Brilliant Blue (CBB) in the single and binary systems. *Adv. J. Chem. Sec. B.* 2: 159-171.
18. Gholami T., Niasari M. S., Varshoy S., (2016), Investigation of the electrochemical hydrogen storage and photocatalytic properties of $CoAl_2O_4$ pigment: Green synthesis and characterization. *Int. J. Hyd. Energy.* 41: 9418-9426.
19. Gonzalez C. J., Calvo M. G., Rivas B. D., Velasco J. R. G., Ortiz J. I. G., Fonseca R. L., (2016), Oxidative steam reforming and steam reforming of methane, isooctane, and N-Tetradecane over an alumina supported spinel-derived nickel catalyst. *Ind. Eng. Chem. Res.* 55: 3920–3929.
20. Josephine B. A., Manikandan A., Teresita V. M., Antony S. A., (2016), Fundamental study of $LaMg_x Cr_{1-x} O_{3-\delta}$ perovskites nano-photocatalysts: Sol-gel synthesis, characterization and humidity sensing. *Korea J. Chem. Eng.* 33: 1590-1598.
21. Padmapriya G., Manikandan A., Krishnasamy V., Jaganathan S. K., Antony S. A., (2016), Spinel $Ni_xZn_{1-x}Fe_2O_4$ ($0.0 \leq x \leq 1.0$) nano-photocatalysts: Synthesis, characterization and photocatalytic degradation of methylene blue dye. *J. Mol. Struc.* 1119: 39-47.
22. Qian X., Li B., Mu H. Y., Ren J., Liu Y., Hao Y. J., Li F. T., (2017), Deep insight into the photocatalytic activity and electronic structure of amorphous earth-abundant $MgAl_2O_4$. *Inorg. Chem. Front.* 4: 1832-1840. 23. Fan J. M., Zhao Z. H., Gong C., Xue Y. Q., Yin S., (2018), Persistent methyl orange degradation ability of Al_2O_4: (Pr^{3+},Dy^{3+})/M-TiO_2 luminescent photocatalyst . *J. Nanosci. Nanotech.* 18: 1675-1681.
24. Sanjabi S., Obeydavi A., (2015), Synthesis and characterization of nanocrystalline $MgAl_2O_4$ spinel via modified sol–gel method. *J. Alloy Compd.* 645: 535–540.
25. Habibi N., Wang Y., Arandiyan H., Rezaei M., (2017), Low-temperature synthesis of mesoporous nanocrystalline magnesium aluminate ($MgAl_2O_4$) spinel with high surface area using a novel modified sol-gel method. *Adv. Powder Technol.* 28: 1249–1257.
26. Rashad M. M., Zaki Z. I., El-Shall H., (2009), A novel approach for synthesis of nanocrystalline $MgAl_2O_4$ powders by co-precipitation method. *J. Mater. Sci.* 44: 2992–2998.
27. Nassar M. Y., Ahmed I. S., Samir I., (2014), A novel synthetic route for magnesium aluminate ($MgAl_2O_4$) nanoparticles using sol–gel auto combustion method and their photocatalytic properties. Spectrochim. *Act. Part A. Mol. Biomol. Spect.* 131: 329–334.
28. Puriwat J., Chaitree W., Suriye K., Dokjampa S., Praserthdam P., Panpranot J., (2010), Elucidation of the basicity dependence of 1-butene isomerization on MgO/$Mg(OH)_2$ catalysts. *Catal. Commun.* 12: 80- 85.
29. Hajavazzade R., Kargarrazi M., Mahjoub A. R., (2019), Phosphotungstic acid supported on $MgAl_2O_4$ nanoparticles as an efficient and reusable nanocatalyst for Benzylic Alcohols oxidation with Hydrogen Peroxide. *J. Inorg. Organomet. Poly Mater.* 29: 1523-1532.
30. Nassar M. Y., Attia A., Alfallous K., El-Shahat M., (2013), Synthesis of two novel dinuclear molybdenum (0) complexes of quinoxaline-2, 3-dione: New precursors for preparation of α-MoO_3 nanoplates. *Inorg Chim. Act.* 405: 362–367.
31. Li H., Liu Y., Tang J., Deng Y., (2016), Synthesis, characterization and photocatalytic properties of $Mg_{1-x}Zn_xAl_2O_4$ spinel nanoparticles. *Solid State Sci.* 58: 14-21.
32. Rahmat N., Yaakob Z., Pudukudy M., Rahman N. A., Jahaya S. S., (2018), Single step solid-state fusion for $MgAl_2O_4$ spinel synthesis and its influence on the structural and textural properties. *Powder Tech.* 329: 409-419.
33. Hajavazzade R., Mahjoub A. R., Kargarrazi M., (2019), Silica-coated $MgAl_2O_4$ nanoparticles supported phosphotungstic acid as an effective catalyst for synthesis of α-aminophosphonates. Res. Chem. Inter. 45: 2341-355.
34. Hajavazzadeh R., Kargar Razi M., Mahjoub A. R., (2019), Aliphatic alcohols oxidation with Hydrogen Peroxide in water catalyzed by supported Phosphotungstic acid (PTA) on Silica coated $MgAl_2O_4$ nanoparticles as recoverable Catalyst. *Int. J. Nano Dimens.* 10: 69-77.
35. Jiang R., Yao J., Zhu H., Fu Y., Guan Y., Xiao L., Zeng G., (2014), Effective decolorization of congo red in aqueous solution by adsorption and photocatalysis using novel magnetic alginate/γ-Fe_2O_3/CdS nanocomposite. *Desali. Water Treat.* 52: 238-247.
36. Jiang R., Zhu H., Fu Y., Jiang S., Zong E., Yao J., (2019), Photocatalytic decolorization of Congo red wastewater by magnetic $ZnFe_2O_4$/Graphene nanosheets composite under simulated solar light irradiation. *Sci. Eng.* 42: 174-182.
37. Hadi Fakhri F., Majeed Ahmed L., (2019), Incorporation CdS with ZnS as nanocomposite and using in photo-decolorization of Congo red dye. *Indones. J. Chem.* 19: 936–943.
38. Kadam R. L., Kim Y., Gaikwad S., Chang M., Tarte H., Han D., (2020), Catalytic decolorization of Rhodamine B, Congo red, and crystal violet dyes, with a novel Niobium Oxide anchored Molybdenum (Nb–O–Mo). *Catalysts.* 10: 491-498.
39. Lei Y. Z., Zhao G. H., Liu M. C., Zhang Z. N., Tong X. L., Cao T. C., (2009), Fabrication, characterization, and photoelectrocatalytic application of ZnO nanorods grafted on vertically aligned TiO_2 nanotubes. *J. Phy. Chem. C.* 113: 19067–19076.
40. Li F. T., Zhaoa Y., Liua Y., Haoa Y. J., Liua R. H., Zhaob D. S., (2011), Solution combustion synthesis and visible light-induced photocatalytic activity of mixed amorphous and crystalline $MgAl_2O_4$ nanopowders. *Chem. Eng. J.* 173: 750-759.